Ultraviolet Laser Footprinting of Histone H1°−Four-Way Junction DNA Complexes†

Dimitri Angelov,‡,§ Emil Novakov,|| Saadi Khochbin,⊥ and Stefan Dimitrov*,‡

Laboratoire de Biologie Moléculaire et Cellulaire de la Différenciation, équipe Mécanismes d'Assemblage du Matériel Génétique et équipe Structure de la Chromatine et Régulation des Gènes, INSERM U 309, Institut Albert Bonniot, Domaine de la Merci, 38706 La Tronche, Cedex, France, et Laboratoire d'Instrumentation Micro-électronique et Informatique, Université Joseph Fourier, B.P. 53, 38041 Grenoble, France

Received March 5, 1999; Revised Manuscript Received June 11, 1999

ABSTRACT: We have used a new light footprinting technique to study the interaction of histone H1° and a deletion mutant δCH1° (lacking H1° COOH-terminal domain) with a synthetic four-way junction DNA. This technique is based on a single 5-ns UV laser pulse and has the ability to map protein−DNA interactions within unperturbed complexes at time scales far faster than molecular rearrangements. We found both H1° and δCH1° to affect the photoreactivity of specific guanine residues located on the central part of four-way junction DNA. These observations demonstrate specific recognition of H1° for the central domain of four-way junction DNA. In addition, histone H1° decreases the photorectivity of selected guanines located some distance from the crossover, indicating specific involvement of the H1° COOH-terminal tail with this region. Immunofractionation of δCH1°−four-way DNA junction complexes with monoclonal anti-H1° antibody combined with the UV laser footprinting method demonstrated the existence of two types of δCH1°−four-way DNA junction complexes.

The first level of chromatin organization in all eukaryotes is the nucleosome. The nucleosome contains a histone octamer consisting of two molecules each of the core histones H2A, H2B, H3, and H4 and a single molecule of linker histone (H1, H1°, or H5) and about 180 bp of DNA (for review see ref *1*). The structure of the histone octamer has been determined by X-ray crystallography to a resolution of 3.1 Å (*2*). Recently, the X-ray crystal structure of the nucleosome core particle has been solved to 2.8 Å resolution, revealing the details of the DNA wound about the histone octamer surface (*3*). Linker histones are composed of three domains, a central globular domain (GH1/GH5/GH1°) and NH_2 and COOH tails, but their positions within the nucleosome remain a matter of controversy (*4*−*17*). Resolution of this problem would be greatly facilitated by a method capable of detecting linker histone−nucleosome interactions with single base pair resolution (*18*). Unfortunately, the existing footprinting techniques are unable to detect linker histones bound within the nucleosome (*12, 19*).

Four-way junction (4WJ)[1] DNAs have been developed as models of the core structures of cruciform DNA and of Holiday junctions (*20*). The 3D structure of 4WJs is also similar to that of DNA crossovers, and it has been proposed that the converging DNA strands within 4WJ DNA imitate the structure of DNA found at the entrance and exit of the nucleosome. Thus 4WJ DNA has been viewed as a simplified model system for studying linker histone−DNA interactions within chromatin (*21*−*23*). Indeed, it was found by band shift analysis that linker histones interact preferentially with 4WJ DNA, the specificity of interaction being determined by the globular domains of these proteins (*21*−*23*). However, only very weak footprints of H1 can be detected on H1−4WJ DNA complexes by existing high-resolution footprinting techniques (*24*).

Irradiation of nucleic acids with UV light induces several base-specific modifications whose spectrum depends on the local conformation of the nucleic acids (*25*−*28*). Since protein−DNA interactions generally change the local conformation of DNA, UV light can be used as a probing agent for the analysis of such interactions. This method, termed photofootprinting, is based on subsequent mapping of the photolesions by chemical or enzymatic treatments that result in strand breaks at the photodamaged bases (*26, 27, 29*). Photofootprinting has been widely used for studying protein−DNA interactions by using conventional low-intensity UV light sources (*25*−*27, 29*). However, low-intensity UV irradiation techniques are unable to detect histone−DNA interactions (*25*−*28*).

†This work was supported by grants from CNRS (ATIPE grant to S.D.), INSERM (contract 4E006B), and the Region Rhône-Alpes (project Emergence).

* Address correspondence to this author: Tel (33) 4 76 54 94 73; Fax (33) 4 76 54 95 95; E-mail Stefan.Dimitrov@ujf-grenoble.fr.

‡ Laboratoire de Biologie Moléculaire et Cellulaire de la Différenciation, équipe Mécanismes d'Assemblage du Matériel Génétique, Institut Albert Bonniot.

§ Permanent address: Institute of Solid State Physics, Bulgarian Academy of Sciences, 1784 Sofia, Bulgaria.

|| Université Joseph Fourier.

⊥ Laboratoire de Biologie Moléculaire et Cellulaire de la Différenciation, équipe Structure de la Chromatine et Régulation des Gènes, Institut Albert Bonniot.

[1] Abbreviations: 4WJ, four-way junction; EDTA, ethylenediaminetetraacetic acid; SDS, sodium dodecyl sulfate; IPTG, isopropyl β-D-thiogalactopyranoside.

10.1021/bi9905260 CCC: $18.00 © 1999 American Chemical Society
Published on Web 08/10/1999

High-intensity UV laser irradiation has several important advantages over conventional sources using low-intensity irradiation techniques for probing the conformation of nucleic acids and protein−DNA interactions both in vivo and in vitro (for review see ref *30*). The laser strategy is based on the rapid single nano- or picosecond laser pulse irradiation of the nucleoprotein samples, which results in irreversible photoreactions. In this way, the existing protein−DNA interactions can be "frozen" and then further examined by molecular biology and immunochemical techniques (*31*−*33*). The UV laser photolesions are induced by a biphotonic mechanism, characteristic for high-intensity irradiation (*28, 30, 31*). A well-documented high-intensity lesion specific for guanine is oxazolone (*34, 35*). This lesion is very sensitive to the local conformation of the DNA helix and is formed upon deprotonation of the initial guanine cation radical (*34*). Treatment with hot piperidine causes quantitative elimination of oxazolone and induces DNA strand breaks at the sites of these guanine modifications (*34*). The strand breaks can be further visualized by polyacrylamide gel electrophoresis under denaturing conditions (*35*).

This paper describes application of a novel UV laser photofootprinting approach to the detection of linker histone−DNA interactions within the H1°−4WJ DNA complex as a model of interactions at the DNA entry/exit point within the nucleosome. By using the laser footprinting technique, we detected a clear footprint of H1° on the central part of 4WJ DNA. Combining this analysis with an immunochemical fractionation procedure, we found that a H1° mutant lacking the C-terminal tail (δCH1) has both a specific and a nonspecific mode of interaction with 4WJ DNA. Only within the specific δCH1°−4WJ DNA complex does δCH1° recognizes the central crossover within the 4WJ DNA.

EXPERIMENTAL PROCEDURES

Preparation of Recombinant Histone H1°. Mouse full-length histone H1° cDNA (*36*) or a cDNA lacking the sequence encoding the C-terminal domain of the protein was cloned in a pET expression vector (Novagen). The expression of the recombinant H1° and C-terminal domain-less H1° (δCH1°) were induced by 1 mM IPTG. Cell were harvested and sonicated. After centrifugation for 10 min at 20000*g*, the supernatant was treated with 5% perchloric acid overnight at 4 °C and centrifuged for 20 min at 20000*g*. The soluble fraction was precipitated with 20% (final concentration) TCA (trichloroacetic acid) and the pellet was washed first with acetone and 1 mM HCl, followed by washing with acetone only. The pellet was air-dried and dissolved in distilled water.

Synthesis of the Four-Way Junctions. The four-way junction DNA was constructed as described (*37*). The four oligonucleotides (ss1, ss2, ss3, and ss4) were synthesized, purified on a 20% sequencing gel, and then radiolabeled with [γ-^{32}P]ATP and T4 polynucleotide kinase by standard procedures. To remove any preexisting oxidative damages, the labeled nucleotides were treated with 1 M piperidine for 30 min at 90 °C and repurified on a 15% polyacrylamide sequencing gel. After electroelution of the oligonucleotides, 4WJs were assembled as follows: 5 pmol of the ^{32}P-labeled oligonucleotide was mixed in 10 mM Tris-HCl, pH 8.0, 1 mM EDTA, and 100 mM NaCl with 10 pmol of the three remaining cold oligonucleotides in a final volume of 50 μL. The reaction was heated for 3 min at 95 °C, allowed to anneal for at least 6 h at 37 °C, and then cooled to room temperature for an additional 2−3 h. The efficiency of cruciform assembly was checked on 8% polyacrylamide native gels.

Assembly of H1°−4WJ DNA Complexes and Electrophoretic Mobility Shift Analysis. Increasing amounts of H1° or δCH1° were incubated with 0.05 pmol of labeled four-way junctions in 20 μL of binding buffer (10 mM Tris-HCl, pH 8, 15 mM NaCl, 5% Ficoll, and 50 μg/mL sonicated DNA from herring sperm) at room temperature for 30 min. The assembled complexes were then analyzed on preelectrophoresed 4% polyacrylamide gels containing 50 mM Tris base and 50 mM glycine (pH 8.9). Electrophoresis was performed at 4 °C. The monoclonal anti-H1° antibody used recognizes amino acids 20−30 within H1° (*38*). Antibody/H1°−4WJ DNA experiments were performed essentially as above. The antibody was added after 15 min of incubation of H1° (δCH1°) and 4WJ DNA, and the incubation was carried out for an additional 15 min before analysis.

Laser Irradiation. The samples (usually 10 μL) were UV-irradiated in siliconized 0.65 mL Eppendorf tubes with a single pulse from the fourth harmonic (266 nm) of a Surelite II (Continuum) Nd−YAG laser (maximum energy 60 mJ, pulse duration 5 ns). The diameter of the laser beam was adjusted to fit that of the sample surface by means of a set of circular diaphragms. The pulse energy of radiation was measured with a calibrated pyroelectrical detector (Ophir Optronics Ltd.) using an 8% deviation beam splitter. The irradiation dose (the pulse energy divided by the beam surface) did not exceed 1 kJ/m^2 [this dose has been previously determined as required for a 35 bp DNA "single hit" experiment (*35*)].

Determination of the Yield of Lesions at Individual Site. After irradiation, the samples were treated with 1 M piperidine for 30 min at 90 °C. The piperidine was removed by five successive evaporations in a speed-vac: each time the dried material was redissolved in 30 μL of H_2O. Finally, the samples were dissolved in 3 μL of formamide loading buffer (deionized formamide, containing 1 mM EDTA, 0.1% xylene cyanol, and 0.1% bromphenol blue), and heated for 3 min at 90−95 °C. The samples were run on 15% sequencing gels (20:1 ratio of acrylamide:bisacrylamide). The gels were then dried and exposed overnight on a PhosphorImager screen.

The quantum efficiency, Q_i, of a lesion at an individual base is defined as $Q_i = R_i/\sigma E R_0$, where R_i/R_0 is the ratio between the amount of the radioactivity R_i in band i and the total radioactivity R_0 loaded within the lane, E is the dose of irradiation (expressed in photons per square centimeter), and σ is the absorption cross-section ($\sigma = 2.3 \times 10^{-17}$ cm^2). R_0 and R_i were determined by integration by using Image Quant version 4.0 Software (Molecular Dynamics). Footprinting results are presented as histograms with height equal to the quantum efficiency at each position along the DNA. The reproducibility of guanine cleavage from several independent experiments was found to be greater than 95%.

RESULTS

Binding of H1° and δCH1° to 4WJ DNA. This study was carried out with recombinant proteins. Figure 1A shows that the isolated recombinant H1° and δCH1° were purified to

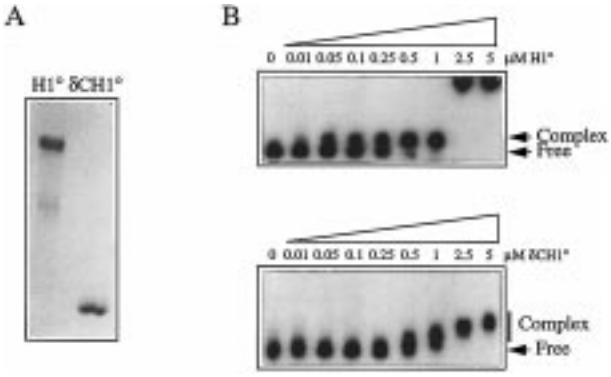

FIGURE 1: Titration of binding of histone H1° and δCH1° to 4WJ DNA. (A) Recombinant histone H1° and δCH1° were purified and run on a 18% polyacrylamide gel containing SDS. (B) ^{32}P-Labeled 4WJ DNA was incubated with increasing amounts of H1° and δCH1° and complexes were separated on a 4% native polyacrylamide gel. The positions of both free and protein-complexed 4WJ DNA are shown.

homogeneity. Titration of 4WJ DNA with H1° led to the assembly of a single H1°−4WJ DNA complex (Figure 1B). At higher histone H1° to 4WJ DNA ratios, aggregates were formed that did not enter the gels. The binding of δCH1° differed from that of the intact protein (Figure 1B). Increasing the concentration of δCH1° resulted in the formation of complexes with reduced mobility. These results are in agreement with published data (*22*).

Binding of H1° and δCH1° to 4WJ DNA Affects Selectively the Photoreactivity of 4WJ DNA Guanine Residues. H1°− and δCH1°−4WJ DNA complexes were assembled on 4WJ DNA in which each strand was individually labeled. A control containing naked 4WJ DNA and the protein−4WJ DNA complexes were irradiated with a single 5-ns pulse, treated with hot piperidine, and separated on sequencing gels as described. Comparison with Maxam−Gilbert G-specific reactions allowed the identification of cleavage positions. The control nonirradiated DNA shows a very low background (Figure 2). However, hot piperidine treatment of the irradiated 4WJ DNA led to the induction of sharp bands with different intensities located essentially on the guanine residues. The presence of H1° as well as δCH1° resulted in a decrease in the intensities of some specific bands, located in all cases around the central part of the 4WJ DNA (Figure 2A−D). This effect was increased upon increasing the protein/4WJ DNA ratio. In the case of H1°−4WJ DNA complexes, the photoreactivity of guanine residues 4 and 5 from 4WJ DNA strand 1 (4WJ1), 9 and 10 from strand 2 (4WJ2), 6 from strand 3 (4WJ3), and 6 and 7 from strand 4 (4WJ4) were particularly sensitive (Figures 2A−D and 3A). A less significant decrease in the photoreactivity of guanine residue 2 from 4WJ1 and 4, 5, and 8 from 4WJ4 was also measured. It should be noted that histone H1° does not affect the guanine residue photoreactivity of the single-stranded oligonucleotides used for assembly of the complete 4WJ DNA (Figure 2E). Similar lack of effect of histone H1 on guanine resudue photoreactivity of these oligonucleotides but in double-stranded form was also observed (Figure 2E). Thus, all the above-described data suggest that the guanine photoreactivity changes found within the H1°−4WJ DNA complexes are determined by the specific interactions of histone H1° with 4WJ DNA.

For δCH1°−4WJ DNA, a decrease in the guanine photoreactivity of 4WJ1, 4WJ2, and 4WJ4 was detected at the same positions as for the strongly affected H1°−4WJ guanine residues. However, in contrast to the significant diminution in the photoreactivity of 4WJ3 guanine 6 observed in the H1°−4WJ DNA complex, little change in the reactivity of this position was detected in the δCH1°−4WJ DNA complex. Additionally, the smaller photoreactivity decrease for guanines located toward the ends of 4WJ1 and 4WJ4 was also absent in δCH1°−4WJ complexes (Figures 2A−D and 3B).

Different Complexes Are Formed upon Binding of δCH1° to 4WJ DNA. The relative decrease in the photoreactivity of centrally located guanine residues within the δCH1°−4WJ DNA complexes was less apparent compared to that of H1°−4WJ DNA complexes (Figure 3). At least two different reasons may be envisaged for the observed difference, the first being related to an effect due to the absence of the H1° C-terminal domain in the δCH1°−4WJ DNA complexes, and the second reflecting different types of interactions of the δCH1°molecules with 4WJ DNA within these complexes. To test the latter hypothesis, we immunofractionated δCH1°−4WJ DNA complexes by a band shift assay (*38*), using a monoclonal antibody that recognizes amino acids 20−30 from the globular domain of histone H1° (Figure 4; see also ref *38*). We first determined the conditions for a complete shift of the 4WJ DNA upon adding δCH1°. Importantly, at this δCH1° to 4WJ DNA ratio essentially the first retarded δCH1°−4WJ DNA complex formed is observed. We further titrated the complex with increasing amounts of the monoclonal antibody and carried out the band shift analysis. The interaction of the antibody with the complex resulted in both the generation of a supershifted fraction (ss), reflecting most probably a ternary δCH1°−4WJ DNA−antibody complex, and dissociation of the complex and release of free DNA (rl, released fraction). This result suggested that at least two different δCH1°−4WJ DNA complexes may coexist that are differentially affected by antibody binding. The possibility of the two types of complexes was further investigated by UV laser footprinting. The assembled δCH1°−4WJ DNA complexes were irradiated with a single 266 nm laser pulse and the irradiated complexes were immunofractionated by band shift. The supershifted fraction and the released fraction were eluted from the gel and their DNA was purified. After hot piperidine treatment, the DNA cleavage products were separated on a sequencing gel and quantified as described under Experimental Procedures. The results are presented in Figure 5. Interestingly, only the released fraction revealed a strong decrease in the photoreactivity of the specific guanine bases as was observed in studies of bulk complexes. Additionally, the extent of the decrease in the photoreactivity of the specific guanines approximates that found in the H1°−4WJ DNA complexes.

DISCUSSION

In this study, we describe the development and use of a novel footprinting approach for studying linker histone−4WJ DNA interactions. The approach is based on the irradiation with a single 5-ns high-intensity laser pulse of the protein−DNA complexes. Such irradiation induces laser-specific biphotonic lesions, whose quantum yield is strongly dependent on the local conformation of DNA. Thus, by measuring

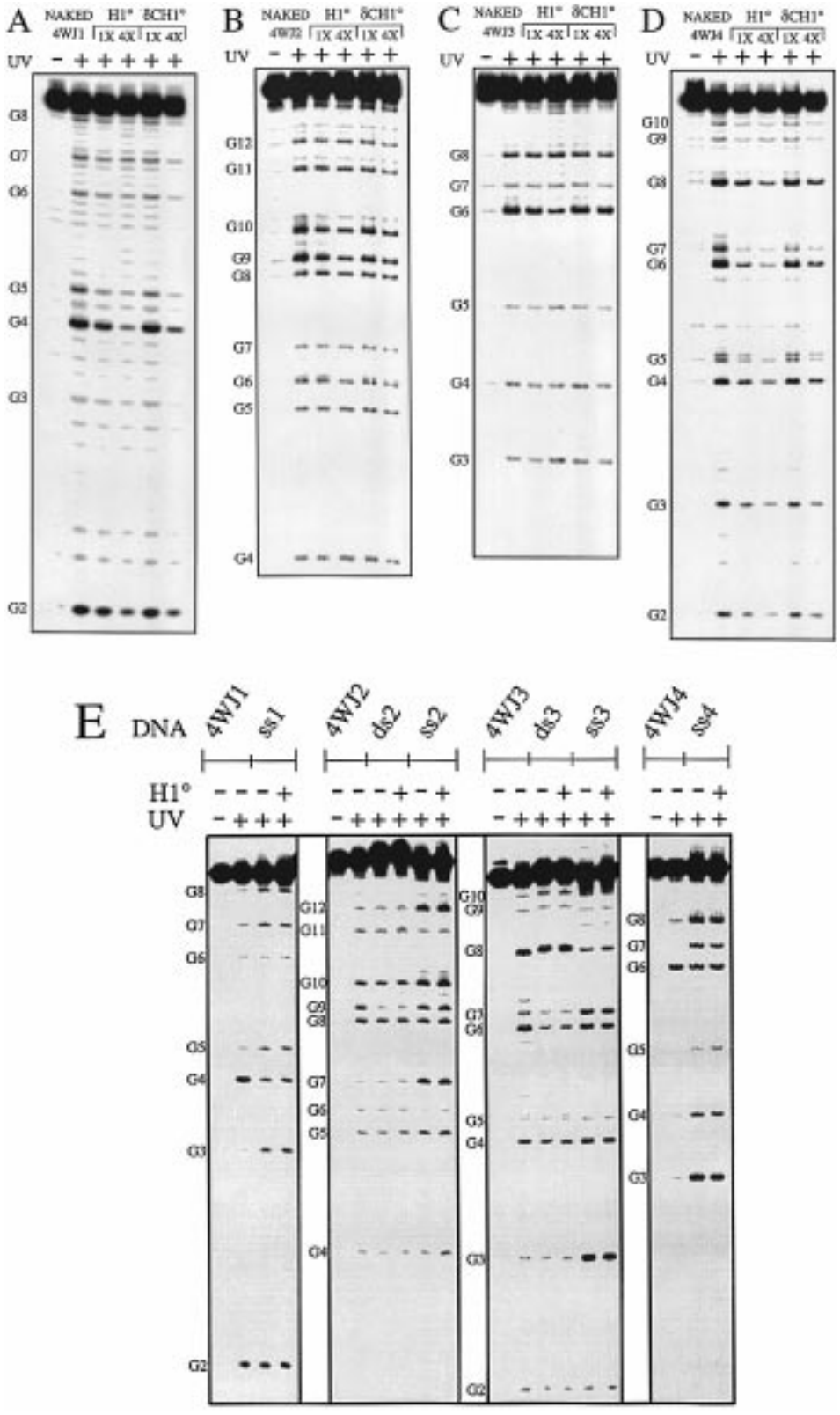

FIGURE 2: UV laser footprinting of H1°−4WJ DNA and δCH1°−4WJ DNA complexes. (A) 4WJ DNA containing 5′-labeled strand 1 (4WJ1) was complexed with either histone H1° or δCH1° and irradiated with a single 266 nm laser pulse. The irradiated samples were then treated with hot piperidine and the cleaved products were separated on a sequencing gel. The pattern of cleavage for nonirradiated (−) and irradiated (+) naked 4WJ DNA are also shown. The positions of the guanine residues are indicated. Panels B−D are the same as panel A, except that within H1° and δCH1° complexes, the 5′-labeled strand is 2 (4WJ2), 3 (4WJ3), or 4 (4WJ4), respectively. 1× and 4× correspond to H1° and δCH1° concentrations of 0.6 and 2.5 μM (see Figure 1). (E) Four different single-stranded 5′-labeled oligonucleotides (ss1, ss2, ss3, and ss4 for strands 1−4, respectively) used for the assembly of 4WJ DNA and the double-stranded oligonucleotides ds2 and ds3, corresponding to strands 2 and 3 of 4WJ DNA (with 5′ end of ss2 and ss3 labeled) were incubated with 2.5 μM H1° and irradiated with a single pulse. The pattern of hot piperidine cleavage for nonirradiated (−) and irradiated single- and double-stranded oligonucleotides, as well as that of naked 4WJ DNA, are shown for comparison.

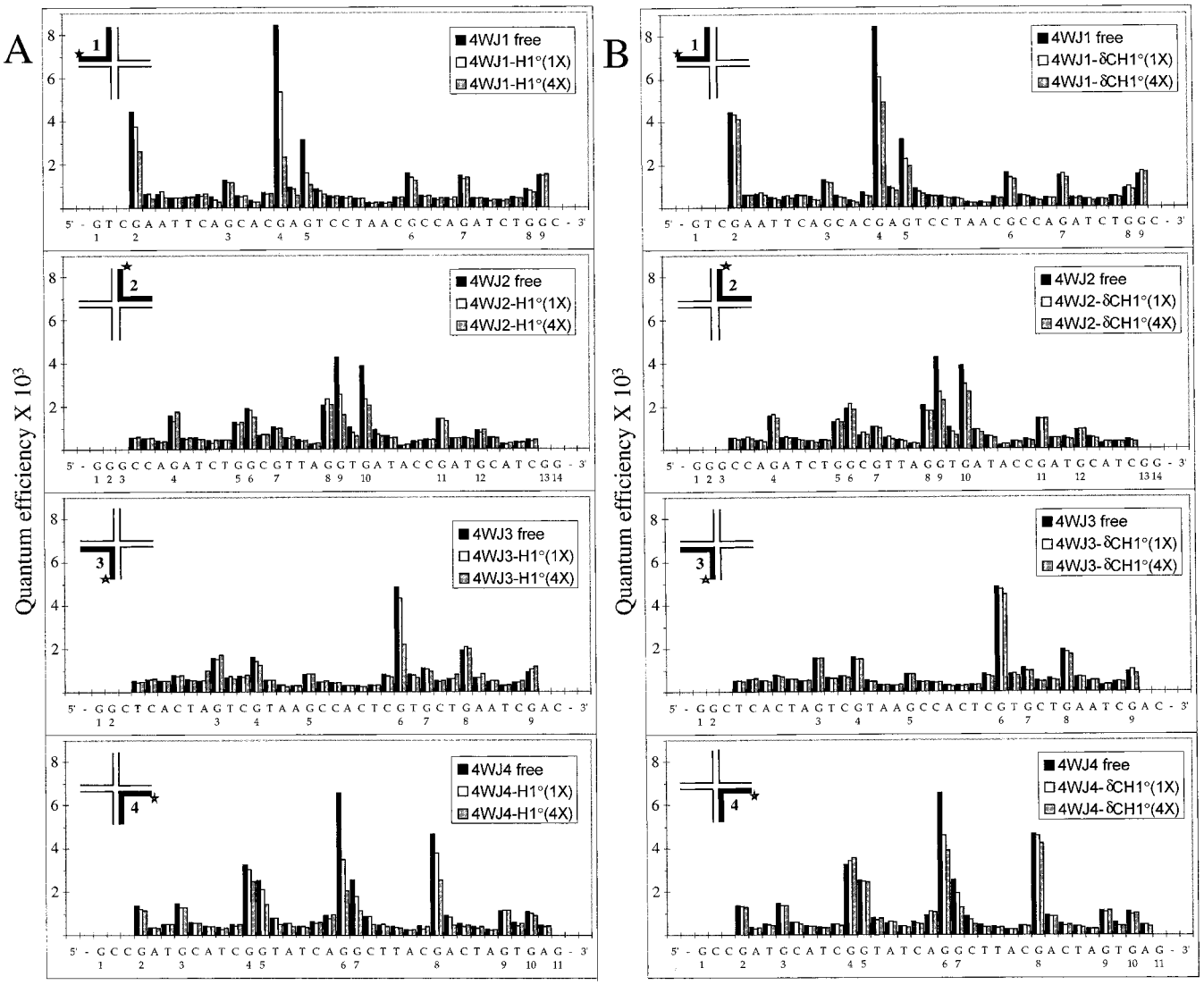

FIGURE 3: Quantum efficiency for lesions detected by hot piperidine treatment for (A) H1°−4WJ DNA complexes and (B) δCH1°−4WJ DNA complexes irradiated with a single 266 nm laser pulse. 1× and 4× correspond to H1° and δCH1° concentrations of 0.6 and 2.5 μM, respectively.

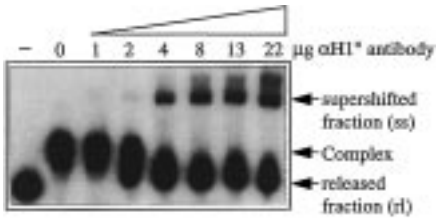

FIGURE 4: Titration of δCH1°−4WJ DNA complexes with the anti-H1° monoclonal antibody. δCH1°−4WJ DNA complexes were incubated with increasing amounts of anti-H1° antibody and analyzed on a 4% native polyacrylamide gel. The positions of the antibody-supershifted δCH1°−4WJ DNA complex (ss), the δCH1°−4WJ DNA complex, and the antibody-released fraction (rl) are shown. (−) indicates the line corresponding to the migration of free 4WJ DNA.

the differences in the quantum lesion efficiency between free and protein-complexed DNA, the binding of a protein may be detected, even if this binding induces very slight changes in the local DNA conformation. Since the footprint is induced by a single laser pulse, the approach could be used also to follow the kinetics of protein−DNA interactions.

We focused our efforts in quantifying oxazolone, a specific biphotonic guanine photolesion, since the mechanism of oxazolone formation is well understood and simple treatment with hot piperidine induces quantitative cleavage at the site of this guanine modification (*34*, *35*). We studied two types of complexes: H1°−4WJ DNA and δCH1°−4WJ DNA. Comparison of the oxazolone formation for these two complexes allowed us to estimate contribution of the different H1° domains to its footprint on 4WJ DNA. We found that the photoreactivity of essentially all guanine residues located at the central part of 4WJ DNA is particularly affected by H1° or δCH1° binding (see Figures 2 and 3). A relatively smaller decrease in photoreactivity was observed for some guanine residues near the ends of 4WJ1 (guanine 2) and 4WJ4 DNA (guanines 4, 5, and 8). These results suggest that histone H1° may recognize the central part of 4WJ DNA (see Figure 6). A similar conclusion was recently reported by Hill and Reeves (*24*), but it was made on indirect data. By use of hydroxyradical footprinting these authors have demonstrated a specific interaction of HMG-I(Y) with the central part of 4WJ DNA. By performing band shift competition experiments they have found that histone H1 directly competes with HMG-I(Y) for the same site on 4WJ DNA and that their binding was mutually exclusive.

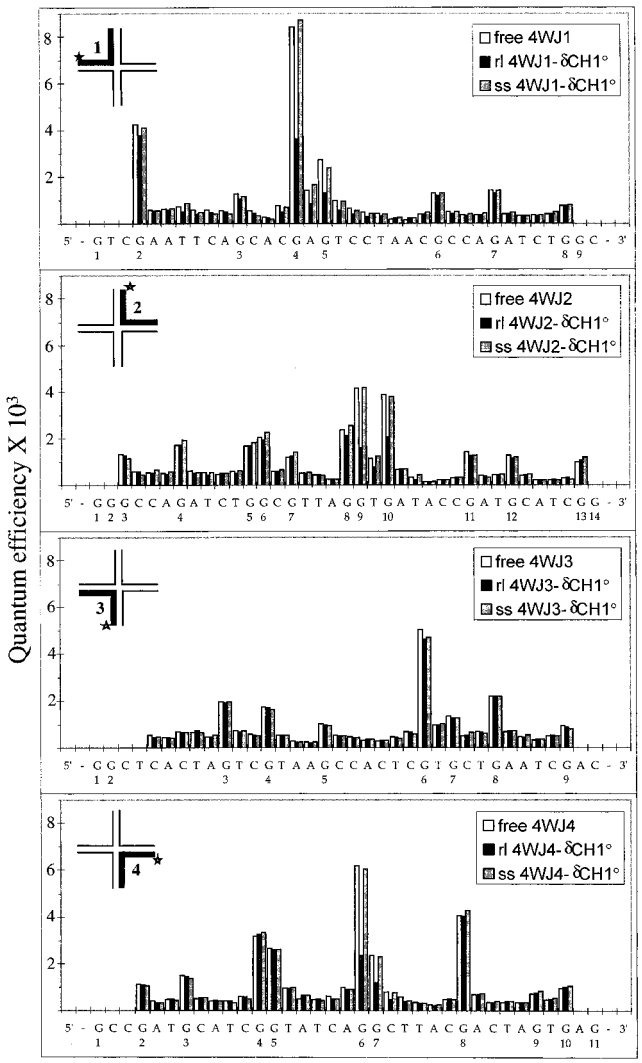

FIGURE 5: Quantum efficiency of lesions within the antibody-supershifted (ss) and antibody-released (rl) fractions from δCH1°−4WJ DNA complexes. After irradiation of the δCH1°−4WJ DNA complexes with a single laser pulse, they were treated with the anti-H1° monoclonal antibody and separated on a 4% native polyacrylamide gel. The supershifted and the released fractions were excised from the gel, electroeluted, cleaved with hot piperidine, and separated on a 15% polyacrylamide sequencing gel, and base photoreactivity was quantified.

Bearing in mind that specific band shifts of 4WJ DNA were observed with the globular domain of linker histones only (*22*), we further examined by laser footprinting which guanine residues were affected in the complexes of 4WJ DNA with a mutant of H1° (δCH1°), lacking the C-terminal tail of H1°. We found that guanines near the ends of the 4WJ DNA, showing a decreased photoreactivity in H1°−4WJ DNA complexes, were not affected in δCH1°−4WJ DNA complexes. Surprisingly, the centrally located guanine 6 of 4WJ3 also showed no changes in photoreactivity as a result of δCH1° binding (see Figure 5). Our interpretation of these data is that δCH1° recognizes the central part of 4WJ1, 4WJ2, and 4WJ4 and induces structural deformations detectable with the laser footprinting. Additionally, the whole histone H1° interacts strongly with the central domain of 4WJ3 (4WJ3 guanine 6 is affected) and it is also responsible for the lower oxazolone formation from the guanines located toward the ends of 4WJ1 and 4WJ4 (Figure 6). Since the C-terminal tail of H1° is very rich in lysines and arginines

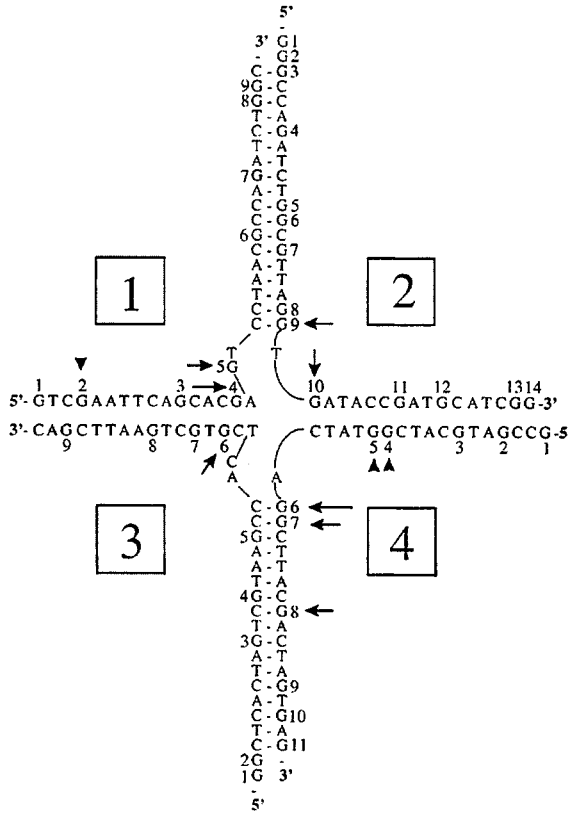

FIGURE 6: Schematic representation of the interaction of H1° with 4WJ DNA. Arrowheads show the guanine bases with decreased photoreactivity resulting from histone H1° binding. The length of the arrow is proportional to the extent of decreased guanine base photoreactivity.

and is quite long, it could easily reach the 4WJ DNA ends and could also contact the central part of 4WJ DNA.

As discussed above, the footprint of δCH1° was detected in the central part of 4WJ DNA but it is also less apparent compared to that of intact H1°. The band shift immunofractionation with the help of the monoclonal antibody showed the existence of at least two different types of complexes, one of which seemed to be specific (it gave the same footprint as the nonfractionated complex) and another one that did not show a footprint. The photoreactivity changes of the guanine residues within the specific complexes were stronger compared to those of the nonimmunofractionated ones. Obviously, within the latter set of complexes the δCH1° footprint was masked by the presence of the nonspecific δCH1°−4WJ DNA interactions. These data suggest that one should be very cautious when discussing the specificity of linker histone−DNA interactions based solely on band shift experiments (*21*−*23*).

The novel light footprinting technique described in this work has major advantages over the existing time-resolved UV laser footprinting approaches (*39*−*41*). For example, the latter methods used primer extension techniques and they are based on the assumption that DNA photolesions (including protein−DNA cross-links) should stop the polymerization reaction of T7 DNA polymerase or of Klenow fragment (*39*−*41*). However, the mechanism of the DNA photolesion-induced inhibition of the polymerization reaction is still ill-defined and whether this inhibition is quantitative remains an open question. On the contrary, our light footprinting approach is based on the cleavage of the well-documented

laser oxidative lesion oxazolone (*34*, *35*), which allows a very precise quantification. Oxazolone is a biphotonic lesion and it strongly depends on the local conformation of DNA, which makes the approach very sensitive, and it has allowed us to describe the footprint of histone H1 on 4WJ DNA.

ACKNOWLEDGMENT

We thank Dr. Jean-Jacques Lawrence for support throughout the course of this work.

REFERENCES

1. van Holde, K. (1988) *Chromatin*, Springer-Verlag, Berlin.
2. Arents, G., Burlingame, R. W., Wang, B.-C., Love, W. E., and Moudrianakis, E. N. (1991) *Proc. Natl. Acad. Sci. U.S.A. 88*, 10148−10152.
3. Luger, K., Mäder, A. W., Richmond, R. K., Sargent, D. F., and Richmond, T. J. (1997) *Nature 389*, 251−260.
4. Thoma, F., Koller, T., and Klug, A. (1979) *J. Cell Biol. 83*, 403−427.
5. Allan, J., Hartman, P. J., Crane-Robinson, C., and Aviles, F. X. (1980) *Nature 288*, 675−679.
6. Simpson, R. T. (1980) *Biochemistry 17*, 5524−5531.
7. Staynov, D. Z., and Crane-Robinson, C. (1988) *EMBO J. 7*, 3685−3691.
8. Thomas, J. O., Rees, C., and Finch, J. T. (1992) *Nucleic Acids Res. 20*, 187−194.
9. Pruss, D., Bartholomew, B., Persinger, J., Hayes, J., Arents, J., Moudrianakis, E. N., and Wolffe, A. P. (1996) *Science 274*, 614−617.
10. Hayes, J. J., Pruss, D., and Wolffe, A. P. (1995) *Proc. Natl. Acad. Sci. U.S.A. 91*, 7817−7821.
11. Hayes, J. J. (1996) *Biochemistry 35*, 11931−11937.
12. Nightingale, K. P., Pruss, D., and Wolffe, A. P. (1996) *J. Biol. Chem. 271*, 7090−7094.
13. Zhou, Y.-B., Gerchman, S. E., Ramakrishnan, V., Travers, A., and Muyldermans, S. (1998) *Nature 395*, 402−405.
14. Travers, A. (1999) *Trends Biochem. Sci. 24*, 4−7.
15. Bradbury, E. M., Chapman, G. E., Danby, S. E., Hartman, P. G., and Riches, P. L. (1975) *Eur. J. Biochem. 57*, 521−528.
16. Ramakrishnan, V., Finch, J. T., Graziano, V., Lee, P. L., and Sweet, R. M. (1993) *Nature 362*, 219−223.
17. Goytisolo, F. A., Gershman, S.-E., Yu, X., Rees, C., Graziano, V., Ramakrishnan, V., and Thomas, J. O. (1996) *EMBO J. 15*, 3421−3429.
18. Crane-Robinson, C. (1997) *Trends Biochem. Sci. 22*, 75−77.
19. Nightingale, K., Dimitrov, S. I., Reeves, R., and Wolffe, A. P. (1996) *EMBO J. 15*, 548−561.
20. Lilley, D. M. J. (1992) *Nature (London) 357*, 282−283.
21. Varga-Weisz, P., van Holde, K., and Zlatanova, J. (1993). *J. Biol. Chem. 268*, 20699−20700.
22. Varga-Weisz, P., Zlatanova, J., Leuba, S. H., Schroth, G. P., and van Holde, K. (1994) *Proc. Natl. Acad. Sci. U.S.A. 91*, 3525−3529.
23. Zlatanova, J., and van Holde, K. (1996) *Prog. Nucleic Acids Res. Mol. Biol. 52*, 217−259.
24. Hill, D. A., and Reeves, R. (1997) *Nucleic Acids Res. 25*, 3523−3531.
25. Becker, M. M., and Wang, J. C. (1984) *Nature 309*, 682−687.
26. Pfeifer, G. P., Drouin, R., Riggs, A. D., and Holmquist, G. P. (1992) *Mol. Cell. Biol. 12*, 1798−1804.
27. Pfeifer, G. P., Drouin, R., and Holmquist, G. P. (1993) *Mutat. Res. 288*, 39−46.
28. Angelov, D., Berger, M., Cadet, J., Marion, C., and Spassky, A. (1994) *Trends Photochem. Photobiol. 3*, 643−663.
29. Becker, M. M., Lesser, D., Kurpiewski, M., Baranger, A., and Jen-Jacobson, L. (1988) *Proc. Natl. Acad. Sci. U.S.A. 85*, 6247−6251.
30. Pashev, I. G., Dimitrov, S. I., and Angelov, D. (1991) *Trends Biochem. S*ci. *16*, 323−326.
31. Angelov, D., Stefanovsky, V. Yu., Dimitrov, S. I., Russanova, V. R., Keskinova, E., and Pashev, I. G. (1988) *Nucleic Acids Res. 16*, 4525−4538.
32. Hockensmith, J. W., Kubasek, W. L., Vorachek, W. R., and von Hippel, P. H. (1986) *J. Biol. Chem. 261*, 3512−3518.
33. Harrison, C. A., Turner, D. H., and Hinkle, D. C. (1982). *Nucleic Acids Res. 10*, 2399−2414.
34. Cadet, J., Berger, M., Douki, T., and Ravanat, J. L. (1997) *Rev. Physiol. Biochem. Pharmacol. 131*, 1−87.
35. Spassky, A., and Angelov, D. (1997) *Biochemistry 36*, 6571−6576.
36. Alonso, A., Breuer, B., Bouterfa, H., and Doenecke, D. (1988) *EMBO J. 7*, 3003−3008.
37. Teo, S. H., Grasser, K. D., Hardman, C. H., Broadhurst, R. W., Laue, E. D., and Thomas, J. O. (1995) *EMBO J. 14*, 3844−3853.
38. Gorka, C., Brocard, M.-P, Curtet, S., and Khochbin, S. (1997) *J. Biol. Chem. 273*, 1208−1215.
39. Buckle, M., Geiselmann, J., Kolb, A., and Buc, H. (1991) *Nucleic Acids Res. 19*, 833−840.
40. Engelhorn, M., Boccard, F., Murtin, C., and Prentki, P. (1995) *Nucleic Acids Res. 23*, 2959−2965.
41. Murtin, C., Engelhorn, M., Geiselmann, J., and Boccard, F. (1998) *J. Mol. Biol. 284*, 949−961.

BI9905260